Using coupling imperfection to control amplitude death

Frank Thomas Ndjomatchoua,[1,*] Byliole S. Djouda,[1] Carlos Lawrence Gninzanlong,[1]
Thierry Landry Michel Mbong Djomo,[2] Maxime Fabrice Kepnang Pebeu,[1] and Clément Tchawoua[1]
[1]*Department of Physics, Faculty of Science, University of Yaoundé 1, P.O. Box 812, Ngoa Ekelle, Yaoundé, Cameroon*
[2]*Department of Civil Engineering, National Higher Polytechnic Institute, University of Bamenda, P.O. Box 39, Bambili, Bamenda, Cameroon*

(Received 20 December 2022; accepted 19 April 2023; published 9 May 2023)

Previous studies of nonlinear oscillator networks have shown that amplitude death (AD) occurs after tuning oscillator parameters and coupling properties. Here, we identify regimes where the opposite occurs and show that a local defect (or impurity) in network connectivity leads to AD suppression in situations where identically coupled oscillators cannot. The critical impurity strength value leading to oscillation restoration is an explicit function of network size and system parameters. In contrast to homogeneous coupling, network size plays a crucial role in reducing this critical value. This behavior can be traced back to the steady-state destabilization through a Hopf's bifurcation, which occurs for impurity strengths below this threshold. This effect is illustrated across different mean-field coupled networks and is supported by simulations and theoretical analysis. Since local inhomogeneities are ubiquitous and often unavoidable, such imperfections can be an unexpected source of oscillation control.

DOI: 10.1103/PhysRevE.107.054207

Understanding networks of coupled oscillator dynamics is a central topic in physics [1–3]. They provide a framework for studying various phenomena in physics and biology [1–3]. Examples from physical science include Josephson junctions [4], populations of chemical oscillators [5], bursting neurons [6], and yeast cells [7]. In particular, the emergence of synchrony, oscillation quenching, and resilience in such networks have received increased attention in recent years [1–3].

Though real-world coupled systems are often heterogeneous, most of the studies are conducted with homogeneous models [1–3]. Heterogeneity plays a central role in coherence resonance enhancement [8], synchronization [9], or signal amplification [10]. Intriguingly, a "single" defect (imperfection or impurity) in a lattice of oscillators enhances the response to a periodic stimulus [11], improves energy harvesting [12], induces the birth and death of breathing modes [13], turns chaotic dynamics into a regular one [14], optimizes wave manipulation [15], or helps in the efficient generation of breathers [16]. The possible role of impurities in oscillation quenching in networks of coupled units remains an open problem and is the object of the present study.

When isolated units oscillate, their dynamics can be quenched if they are adequately coupled [2,3]. There are two distinct types of oscillation quenching processes: amplitude death (AD) and oscillation death (OD). The AD results in a homogeneous steady state (HSS) since all oscillators populate the same state. However, in the case of OD, oscillators populate different coupling-dependent steady states and thus give rise to stable inhomogeneous steady states (IHSSs). Yet, in some circumstances, the cessation of oscillations corresponds to an AD situation with a heterogeneous and stable solution. When connected units with IHSSs have oscillation amplitudes not collapsing into completely new steady states, the phenomenon is classified as AD rather than OD [17]. As a result, whether the quenched steady state is new or not affects the categorization of AD or OD more than whether it is homogenous or inhomogeneous [17]. This remarkable phenomenon is well-established theoretically and experimentally across various lattices and networks in physics, biology, chemistry, and engineering systems [2,3]. The present work is motivated by leveraging impurity to address the problem of quenching control in systems of coupled oscillators.

The problem of oscillation restoration in a network predisposed to AD dynamics has received some attention. It is demonstrated that gradient coupling, processing delay, diffusion self-feedback factors, a linear feedback technique, or a local low-pass filter restore rhythmicity in the corresponding parameter space that naturally induces AD [2,3]. Most of these methods rely on oscillator parameters or attributes of coupling adjustment over the whole network [2,3]. However, our world is extensively made of wide networks whose nodes can be neurons (brain), subjects (social networks, ecology), devices (power grids), and elements (chemical reactions and biological systems). Therefore, simultaneously tuning network properties at all nodes to achieve desired global dynamics can be challenging. Recently, Tamaševičius *et al.* [18] stabilized the entire array of coupled oscillators by deactivating a single accessed (or randomly chosen) unit. This local deactivation propagates to the other network nodes, leading to AD [18]. This article intends to elucidate the role of a local coupling alteration in oscillation restorations.

To investigate the effect of such local alteration, we use a localized defect in the network linkage such that a unique oscillator is coupled differently from others. Contrary to [18], all of the units involved remain identical and have not been

*ftndjomatchoua@gmail.com

purposefully deactivated. Below a threshold impurity strength, the coupling can perturb the steady state of the network, annihilate AD through Hopf's bifurcation, and revive oscillation in the AD regime to retain the sustained rhythmic functioning of the networks. This critical value for oscillation revival is estimated analytically as a function of network size and confronted with numerical simulation.

The first model used as a case study is the Van der Pol oscillator (VDPO) [19]. The VDPOs are networked through a mean-field coupling [20–22]: $\dot{x}_i = y_i + \varepsilon_i(Q\bar{x} - x_i)$; $\dot{y}_i = \kappa(1 - x_i^2)y_i - x_i$. The second model is the Stuart-Landau oscillators (SLO) [23]: $\dot{x}_i = [1 - (x_i^2 + y_i^2)]x_i - \omega y_i + \varepsilon_i(Q\bar{x} - x_i)$; $\dot{y}_i = [1 - (x_i^2 + y_i^2)]y_i + \omega x_i$. The index $i = 1, \ldots, N$ ($N \gg 1$) refers to nodes (oscillators) and $\bar{x} = N^{-1}\sum_1^N x_i$ is the mean field. The coupling strength is given by ε_i. The parameter Q ($0 < Q \leqslant 1$) is the density of the mean field which controls the influence of the mean field on the system dynamics. The impurity (or a defect) coupling is only at one specific node ($\varepsilon \neq \varepsilon_0$), i.e., $\varepsilon_i \equiv [\varepsilon_0, \ldots, \varepsilon_0, \varepsilon, \varepsilon_0, \ldots, \varepsilon_0]$. The parameters ε_0 and Q are selected such that the system converges to a steady state when the network is homogeneous ($\varepsilon = \varepsilon_0$). The parameter ε stands for *impurity strength*, while the remaining $N - 1$ nodes have a same coupling ε_0. The VDPO shows a nearly sinusoidal oscillation for smaller κ and relaxation oscillation for larger κ [19]. For an identical VDPO oscillator with parameters $Q = 0.3$, $\varepsilon_0 = 1.5$, and $\kappa = 0.35$, the coupled systems are expected to be exhibit AD [20–22]. In the absence of the coupling, individual SLO shows an oscillating dynamics for $\omega = 5$. For the values $Q = 0.5$ and $\varepsilon_0 = 5$, the coupled SLO system is in AD [23]. The aim is to find the threshold (or critical) value of ε (ε^{th}) allowing a switch from AD to oscillatory regime.

Analytical method. The standard linear stability is performed to obtain the critical impurity strength [3,20–23]. After linearizing VDPOs and SLOs around the trivial HSS $(x_i^*, y_i^*) = (0{,}0)$, the real parts of the eigenvalues of each Jacobian matrices are equated to 0 and the thresholds

$$\varepsilon_V^{th} = \kappa\frac{N\kappa + N(Q-1)\varepsilon_0 - Q\varepsilon_0}{\kappa(N-Q) + N(Q-1)\varepsilon_0} \tag{1}$$

and

$$\varepsilon_S^{th} = \frac{4N + 2N(Q-1)\varepsilon_0 - 2Q\varepsilon_0}{2(N-Q) + N(Q-1)\varepsilon_0} \tag{2}$$

are obtained for VDPOs and SLOs, respectively. When $\varepsilon < \varepsilon^{th}$ the theory suggests that AD will be annihilated and the oscillations will be reborn. For the coupled VDPOs, the critical value decreases for large N and saturates to $\varepsilon_{V\infty}^{th} = \lim_{N\to\infty}\varepsilon_V^{th} = \kappa$. For the SLO case, the threshold saturates to $\varepsilon_{S\infty}^{th} = 2$. Thus network size plays a crucial role in the oscillation revival criterion for a relatively small-sized network.

The threshold value is numerically estimated and tested by a dichotomic method. Owing the AD occurs when the real part of the largest eigenvalue [Re(LEV)] (i.e., the rightmost eigenvalue in the complex plane) of the Jacobian matrix at the HSS is negative [3]; the Re(LEV) is straightforwardly computed with the usual numerical methods [24]. The expected threshold lies between ε_-^{th} and ε_+^{th}, where Re(LEV) is negative and positive, respectively. The interval $[\varepsilon_-^{th}, \varepsilon_+^{th}]$ is found through brute-force procedure and subsequently refined iteratively by a dichotomic search algorithm, the execution of which is stopped once a precision $|\varepsilon_+^{th} - \varepsilon_-^{th}| < 10^{-14}$ is reached, leading to numerical approximation of $\varepsilon^{th} \approx (\varepsilon_+^{th} + \varepsilon_-^{th})/2$. This supports the validity of the analytical results [Eqs. (1) and (2)] through numerical simulations.

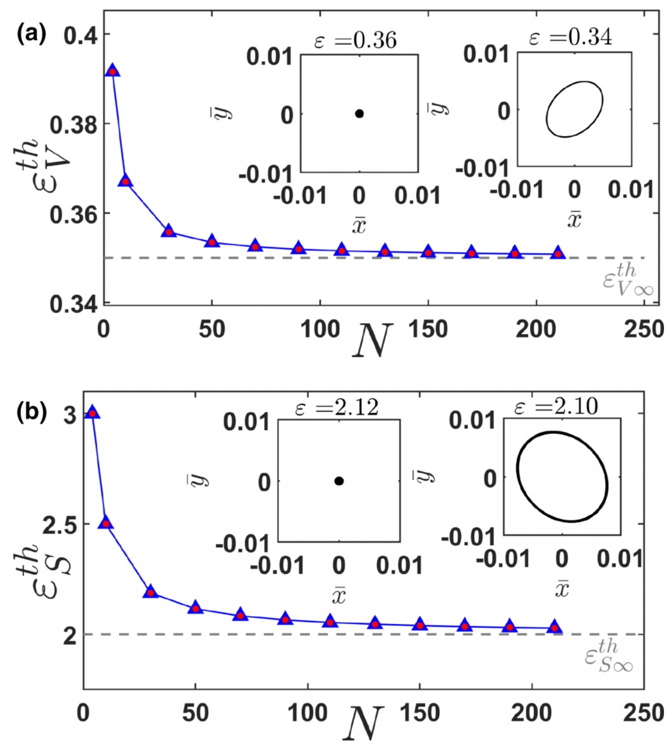

FIG. 1. Comparison between the analytic (blue triangle) and numeric (red dot) values for the impurity strength threshold with different network size for VDPO (a) and SLO (b), respectively. For inner graphics, the network size is $N = 50$ with the impurity at node $i = 25$. The initial conditions $[x_i(0), y_i(0)]$ are randomly and uniformly sampled in the interval $[-1,\ 1]$. The phase portraits $(\bar{x}, \bar{y})$ are obtained from time series of averaged values for 10 randomly selected nodes. In (a), $Q = 0.30$, $\kappa = 0.35$, and $\varepsilon_0 = 1.5$. In (b), $Q = 0.5$, $\omega = 5.0$, and $\varepsilon_0 = 5.0$. The values $\varepsilon_{V\infty}^{th}$ and $\varepsilon_{S\infty}^{th}$ (horizontal gray dashed line) are the asymptotic threshold values for $N \to \infty$ corresponding to VDPO and SLO, respectively.

A match between the numerical and analytical method is observed (Fig. 1). For the VDPO [Fig. 1(a)], $\varepsilon_V^{th} \simeq 0.35$ for the chosen parameters. It can be noticed that, for $\varepsilon = 0.36 > \varepsilon_V^{th}$, the amplitudes of oscillations die out after a sufficiently long time. For $\varepsilon = 0.34 < \varepsilon_V^{th}$ the oscillations are sustained. For the SLO [Fig. 1(b)], $\varepsilon_S^{th} \simeq 2.11$ for the chosen parameters. When $\varepsilon = 2.12 > \varepsilon_S^{th}$, the dynamics is quenched. For $\varepsilon = 2.10 < \varepsilon_S^{th}$ the system shifts to an oscillatory regime. For the VDPO case, the largest eigenvalues (LEVs) are $-0.0034 \pm j0.9355$ ($\varepsilon = 0.36$) and $0.0066 \pm j0.939205$ ($\varepsilon = 0.34$). For the SLO case, the LEVs are $-0.0018 \pm j4.8986$ ($\varepsilon = 2.12$) and $0.0062 \pm j4.90025$ ($\varepsilon = 2.10$), respectively (with $j^2 = -1$). Therefore, when the impurity strength is varied downward below the threshold, the AD state is destabilized through Hopf's bifurcation and the oscillations are revived. The stable HSS region is gradually reduced for decreasing ε. The impurity coupling acts as a feedback and moves the system to the oscillatory state. Hence, depending on the impurity strength, the mean-field coupling suppresses as well as regenerates the oscillation.

Now, we shall illustrate that the impurity ε is also capable of annihilating the onset of AD, which is induced by the birth of a new set of stable IHSS due to the coupling. For this purpose, we consider coupled Brusselator's oscillators (BSLO) [25]: $\dot{x}_i = -(B+1)x_i + x_i^2 y_i + A + \varepsilon_i(Q\overline{x} - x_i)$; $\dot{y}_i = Bx_i - x_i^2 y_i$. In the absence of coupling, each oscillator exhibits limit cycle behavior when $B > A^2 + 1$ [25]. In the presence of the mean-field coupling, an analytical solution (x_i^{eq}, y_i^{eq}) of $\dot{x}_i = 0$ and $\dot{y}_i = 0$ is challenging. To find a value for the steady state, it is first assumed that the trivial solution is identical for all nodes (x_0^*, y_0^*) except for the impurity (x^*, y^*). Therefore,

$$x^* = \frac{-A[NQ\varepsilon + \varepsilon_0(N + Q - NQ) + N - Q\varepsilon]}{\varepsilon_0[N(Q-1)(\varepsilon+1) - Q] - N(\varepsilon+1) + Q\varepsilon}, \quad (3)$$

$$x_0^* = \frac{-A[N\varepsilon + N - Q\varepsilon + Q\varepsilon_0]}{\varepsilon_0[N(Q-1)(\varepsilon+1) - Q] - N(\varepsilon+1) + Q\varepsilon}, \quad (4)$$

$y^* = B/x^*$, and $y_0^* = B/x_0^*$. Starting with an educated guess [Eqs. (3) and (4)], all the exact x_i^{eq} and y_i^{eq} are then determined using equations $\dot{x}_i = 0$ and $\dot{y}_i = 0$ via a standard multidimensional root solver based on the Newton-Raphson method [24]. For analytical tractability, the impurity strength threshold is only found numerically using the dichotomic search procedure. Similar to the HSS cases, the threshold is a decreasing function of the network size and saturates to a constant value at $N \to \infty$ [Fig. 2(a)]. The solution diagrams of the steady states for $\varepsilon > \varepsilon_B^{th}$ and $\varepsilon < \varepsilon_B^{th}$ ($\varepsilon_B^{th} \simeq 5.14243$), respectively, are plotted in Fig. 2(a). The corresponding LEVs shift from $-0.0020 \pm j0.9742$ ($\varepsilon = 5.15$) to $0.0033 \pm j0.9778$ ($\varepsilon = 5.13$), indicating a Hopf's bifurcation through which the stable IHSS loses its stability for decreasing ε below the critical value ε_B^{th}. The presence of impurity ε in the coupling does not change the structure of the steady-state solutions, but just switches their stability [Fig. 2(b)]. In other words, the steady state is not a completely new state induced by the coupling, but a smooth transformation of the original equilibrium of the system, which turns out to be node dependent when the impurity is present. As the steady state associated with OD corresponds to new states created by the coupling [3], the observation that here the fixed point is not new is key to classifying the observed oscillation quenching mechanism as AD rather than OD. This asserts that inhomogeneous AD induced by the coupling can also be destabilized by the impurity for $\varepsilon < \varepsilon_B^{th}$ leading to sustained oscillations.

To go beyond the standard limit-cycle oscillators previously considered, the chaotic Rössler oscillator is considered as an illustrative case. The coupled Rössler oscillators (RLOs) networked through a mean-field coupling are defined as follows [3,26]: $\dot{x}_i = -y_i - z_i + \varepsilon_i(Q\overline{x} - x_i)$, $\dot{y}_i = x_i + ay_i$, and $\dot{z}_i = b + z_i(x_i - c)$. In the absence of the coupling, individual RLO exhibits a chaotic oscillating dynamics for $a = 0.1$, $b = 0.1$, and $c = 18.0$. For the values $Q = 0.4$ and $\varepsilon_0 = 0.2$, the identically coupled RLO system is in AD [3,26]. Starting from the homogeneous stationary state obtained in [26], the *true* steady state for the nonlinear coupled equations $\dot{x}_i = 0$, $\dot{y}_i = 0$, and $\dot{z}_i = 0$ including the impurity is

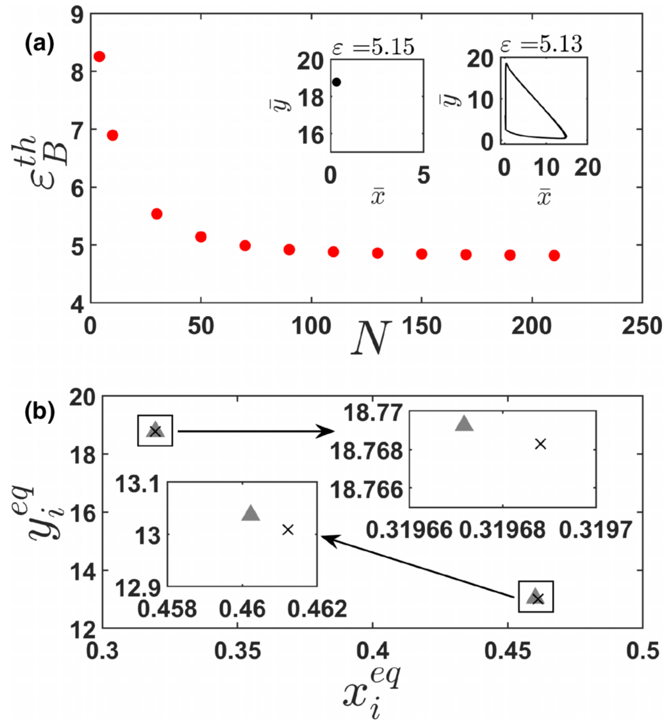

FIG. 2. Values for the impurity strength threshold (red dots) with different network size for BSLO (a). For inner graphics in (a), the network size is $N = 50$ with the impurity at node $i = 25$. The initial conditions $[x_i(0), y_i(0)]$ are the equilibria states x_i^* and y_i^* with added perturbations randomly and uniformly sampled in the interval [0.001,0.01]. The phase portraits $(\bar{x}, \bar{y})$ are obtained from time series of averaged values for 10 randomly selected nodes. In (a), $Q = 0.5$, $A = 2.0$, $B = 6.0$, and $\varepsilon_0 = 10.6061$. In (b), coordinates of the heterogeneous fixed point of $i = 1 \cdots N$ the BSLO system for $\varepsilon = 5.15$ (gray triangles) and $\varepsilon = 5.13$ (black crosses). There are two distinct equilibria for each value of ε: one (1) originating from the impurity, while the second is associated to the identical $(N-1)$ other oscillators. This justifies the two separated points obtained for each parameter ε on the graph. The zooms are applied to distinguish the fixed points obtained below (black crosses) and above (gray triangles) the impurity strength threshold, confirming the preservation of the IHSSs structure after bifurcation.

obtained through the iterative correction procedure previously described.

Similar to the VDPO, SLO, and BSLO systems, the threshold is a decreasing function of the network size and saturates to a constant value at $N \to \infty$ (Fig. 3). The solution diagrams of the steady states for $\varepsilon > \varepsilon_R^{th}$ and $\varepsilon < \varepsilon_R^{th}$ ($\varepsilon_R^{th} \simeq 0.1034$) are plotted in Fig. 3. A very small defect coefficient ($\varepsilon = 0.01$) does not strongly affect the behavior of the uncoupled system, because each oscillator remains chaotic, with a high number and dense orbits in the phase space. Upon increasing the coupling, to $\varepsilon = 0.05$, the oscillators evolve in quasiperiodicity with two orbits in the phase space, but each having a very close limit-cycle amplitude. A further increase of the coupling up to $\varepsilon = 0.10$ induces a periodic behavior in the whole system. Increasing the coupling to $\varepsilon = 0.15$ ($\varepsilon > \varepsilon_R^{th}$), the system reaches a steady state. In a similar manner to the previous models, the Re(LEV) becomes positive below the threshold ε_R^{th}. Thus the destabilization of the steady state

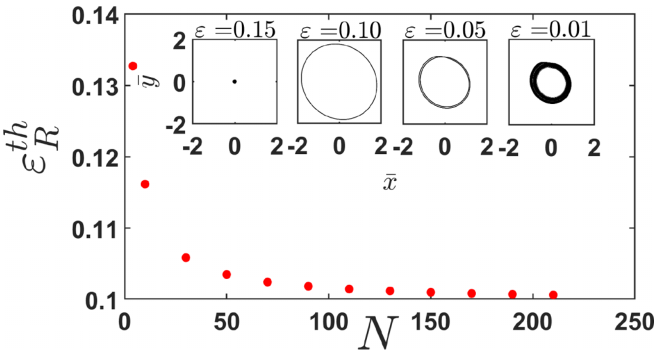

FIG. 3. Values for the impurity strength threshold ε_R^{th} (red dots) with different network size for RLO (a). For inner graphics, the network size is $N = 50$ with the impurity at node $i = 25$. The initial conditions $[x_i(0), y_i(0), z_i(0)]$ are randomly and uniformly sampled in the interval $[-1, 1]$. The phase portraits $(\bar{x}, \bar{y})$ are obtained from time series of averaged values for 10 randomly selected nodes. The parameters used are $Q = 0.40$, $a = 0.1$, $b = 0.1$, $c = 18.0$, and $\varepsilon_0 = 0.2$. For $\varepsilon = 0.01$, the maximum Lyapunov exponent is positive (result not reported here), while it is negative for $\varepsilon = 0.05$, 0.10, and 0.15.

and birth of periodic solution is due to Hopf's bifurcation. Therefore, through a unique impurity, it is possible to suppress AD, control the magnitude of oscillation amplitude, and turn chaotic dynamics into regular oscillation.

Discussion and conclusions. The oscillation revival phenomenon's mechanism is very simple: lowering the coupling ε of one oscillator causes it to enter the oscillatory domain, despite the fact that all of the other $N - 1$ oscillators have parameters that lead to AD (see $Q - \varepsilon$ parameter spaces for oscillatory and AD regimes of homogenous mean-field coupled oscillators depicted in Refs. [19–23]). The current work, however, indicates that picking impurity parameters from the $Q - \varepsilon$ region for oscillation is insufficient. Using the right amount of impurity coupling below a specific threshold can effectively "free" such units from the network and thus restore oscillations. At the beginning of the dynamics, the amplitude of the impurity is notably different from others, but over a long period of time, all of the phases and amplitudes of all oscillators are identical (result not reported here). Then, this perturbed oscillator acts as a common periodic driver for the whole system.

Compared to previous works [3,8–16], we demonstrated that an impurity competes with the quenching effects of mean-field coupling in circumventing the onset of AD. The revival of oscillations by the impurity occurs via Hopf's bifurcation. Therefore, a single impurity can revive or revoke oscillations in the AD parameter regime. This control approach seems simple and more practical compared to linking sophistication or all the networked oscillators at once [3].

Previous attempts to induce AD with impurities relied on the deactivation of a single oscillator [18], in contrast to the present study, where all the subunits remain nondeactivated and a comparable result is obtained.

Though there is a maximum system size N beyond which AD no longer exists in delay-coupled systems, it is independent of N in homogeneous mean-field diffusion. Unexpectedly, the present study demonstrates that size is relevant in the presence of a single impurity. The homogenous version of the models has a threshold independent of the size [20–23,26]; furthermore, in the absence of the impurity, previous results are recovered [20–23,26].

The results of conventional models such as the limit-cycle oscillator and the chaotic oscillator show that the underlying phenomenon is quite general and promising. This approach may be used to control AD in oscillatory systems with mean-field diffusion as a generic mechanism.

Despite the fact that this is a theoretical study, analog electronic-circuit-based experiments in Refs. [20,21] can be used to implement mean-field coupling. While state variables x, y, and z are operational amplifier output voltages, resistors determine system parameters (e.g., κ and ω). Investigation of the effect of impurity strength can be conducted by suitably modifying the resistor governing the coupling at a single node only [20,21]. Since the VDPO, SLO, BLSO, or RLO are ubiquitously encountered in physical systems, the practical utility of such an AD control will be highly context dependent.

This unusual effect of impurity in reviving oscillations could provide a valuable clue to understanding the sustained oscillatory behavior of many natural systems via a local change. We believe the presence of even a single impurity will significantly impact the proper functioning and robustness of large networks such as coupled biological and chemical systems, neural networks, socially interacting species, etc. We anticipate that this study will open the door to further research into the most effective local repair and regeneration techniques for network systems.

[1] S. Boccaletti, J. Kurths, G. Osipov, D. L. Valladares, and C. S. Zhou, The synchronization of chaotic systems, Phys. Rep. **366**, 1 (2002).

[2] T. Stankovski, T. Pereira, P. V. E. McClintock, and A. Stefanovska, Coupling functions: Universal insights into dynamical interaction mechanisms, Rev. Mod. Phys. **89**, 045001 (2017).

[3] W. Zou, D. V. Senthilkumar, M. Zhan, and J. Kurths, Quenching, aging, and reviving in coupled dynamical networks, Phys. Rep. **931**, 1 (2021).

[4] K. Wiesenfeld, P. Colet, and S. H. Strogatz, Synchronization Transitions in a Disordered Josephson Series Array, Phys. Rev. Lett. **76**, 404 (1996).

[5] I. Z. Kiss, Y. Zhai, and J. L. Hudson, Emerging coherence in a population of chemical oscillators, Science **296**, 1676 (2002).

[6] I. Belykh, E. de Lange, and M. Hasler, Synchronization of Bursting Neurons: What Matters in the Network Topology, Phys. Rev. Lett. **94**, 188101 (2005).

[7] S. Danø, F. Hynne, S. De Monte, F. D'Ovidio, P. G. Sorensen, and H. Westerhoff, Synchronization of glycolytic oscillations in a yeast cell population, Faraday Discuss. **120**, 261 (2002).

[8] C. Zhou, J. Kurths, and B. Hu, Array-Enhanced Coherence Resonance: Nontrivial Effects of Heterogeneity and Spatial Independence of Noise, Phys. Rev. Lett. **87**, 098101 (2001).

[9] Y. Sugitani, Y. Zhang, and A. E. Motter, Synchronizing Chaos with Imperfections, Phys. Rev. Lett. **126**, 164101 (2021).

[10] C. J. Tessone, C. R. Mirasso, R. Toral, and J. D. Gunton, Diversity-Induced Resonance, Phys. Rev. Lett. **97**, 194101 (2006).

[11] A. Valizadeh, Enhanced response of regular networks to local signals in the presence of a fast impurity, Phys. Rev. E **86**, 016101 (2012).

[12] M. Hwang and A. F. Arrieta, Input-independent energy harvesting in bistable lattices from transition waves, Sci. Rep. **8**, 3630 (2018).

[13] A. Gómez-Rojas and P. Halevi, Discrete breathers in an electric lattice with an impurity: Birth, interaction, and death, Phys. Rev. E **97**, 022225 (2018).

[14] C. L. Gninzanlong, F. T. Ndjomatchoua, and C. Tchawoua, Taming intrinsic localized modes in a DNA lattice with damping, external force, and inhomogeneity, Phys. Rev. E **99**, 052210 (2019).

[15] H. Yasuda, E. G. Charalampidis, P. K. Purohit, P. G. Kevrekidis, and J. R. Raney, Wave manipulation using a bistable chain with reversible impurities, Phys. Rev. E **104**, 054209 (2021).

[16] X. Liu, M. Wen, X. Mao, and X. Wang, Optimal and efficient generation of sine-Gordon breathers, Phys. Rev. E **104**, 014209 (2021).

[17] P. Clusella, M. C. Miguel, and R. Pastor-Satorras, Amplitude death and restoration in networks of oscillators with random-walk diffusion, Commun. Phys. **4**, 13 (2021).

[18] A. Tamaševičius, S. Bumeliene, and E. Adomaitiene, Using a single deactivated oscillator to stabilize the steady states in an array of coupled FitzHugh–Nagumo cells, Nonlinear Dyn. **106**, 3557 (2021).

[19] A. Jenkins, Self-oscillation, Phys. Rep. **525**, 167 (2013).

[20] T. Banerjee and D. Ghosh, Experimental observation of a transition from amplitude to oscillation death in coupled oscillators, Phys. Rev. E **89**, 062902 (2014).

[21] D. Ghosh, T. Banerjee, and J. Kurths, Revival of oscillation from mean-field-induced death: Theory and experiment, Phys. Rev. E **92**, 052908 (2015).

[22] U. K. Verma, A. Sharma, N. K. Kamal, J. Kurths, and M. D. Shrimali, Explosive death induced by mean–field diffusion in identical oscillators, Sci. Rep. **7**, 7936 (2017).

[23] T. Banerjee and D. Ghosh, Transition from amplitude to oscillation death under mean-field diffusive coupling, Phys. Rev. E **89**, 052912 (2014).

[24] W. H. Press, S. A. Teukolsky, W. T. Vetterling, and B. P. Flannery, *Numerical Recipes in Fortran: The Art of Scientific Computing*, 2nd ed. (Cambridge University Press, Cambridge, UK, 1992).

[25] K. Bar-Eli, On the stability of coupled chemical oscillators, Physica D **14**, 242 (1985).

[26] A. Sharma and M. D. Shrimali, Amplitude death with mean-field diffusion, Phys. Rev. E **85**, 057204 (2012).